Pergamon

Geochimica et Cosmochimica Acta, Vol. 62, No. 3, pp. 393-404, 1998

0016-7037/98 $19.00 + .00

PII S0016-7037(97)00343-8

Testing theoretically predicted stalagmite growth rate with Recent annually laminated samples: Implications for past stalagmite deposition

ANDY BAKER,[1,*] DOMINIQUE GENTY,[2] WOLFGANG DREYBRODT,[3] WILLIAM L. BARNES,[4] NATALIE J. MOCKLER,[1,4] and JIM GRAPES[1]

[1]Department of Geography, University of Exeter, Amory Building, Rennes Drive, Exeter EX4 4RJ, UK
[2]URA 723, CNRS, LGHI, bat. 504, Universite de Paris-Sud, Orsay, France
[3]Institute of Experimental Physics, University of Bremen, 28334 Bremen, Germany
[4]Department of Physics, University of Exeter, Stocker Road, Exeter EX4 4QL, UK

(*Received May* 7, 1997; *accepted in revised form September* 24, 1997)

Abstract—Annually laminated stalagmites deposited over the last 30–160 years are analysed to determine their growth rate. Three natural and artificial cave sites in England, France, and Belgium were chosen for their wide range of variability in growth rate determining variables, and multiple samples were taken from each site. The annual nature of laminae deposition within the stalagmite calcite was confirmed by comparison to the date of cave/void opening, ^{14}C analyses, or by using dated event horizons. Measured stalagmite growth rate was determined from annual laminae thickness measurements and compared to that theoretically predicted from the chemical kinetics of the calcite precipitation reaction. A good agreement is observed between empirical observations and theoretical predictions, although two complicating factors, variations in calcite porosity, and seasonal cessation of the water supply to the samples, both affect the growth rate. Implications for the extraction of palaeoclimate information from stalagmite growth rate are discussed. *Copyright © 1998 Elsevier Science Ltd*

1. INTRODUCTION

The mechanisms and rate of stalagmite growth have been investigated for over 30 years. Franke (1965) demonstrated how stalagmite shapes vary due to the deposition process, postulating that increased drip rate would lead to an increase in stalagmite diameter. Curl (1973) presented a theory to explain the formation of minimum diameter stalagmites based on physics principles, while Gams (1981) investigated the effect of fall height on stalagmite diameter. Empirical studies of the rate of stalagmite growth rate has involved utilising markers on the surfaces of stalagm-Holme, 1863; Hovey, 1896; Prinz, 1908) or by using microscope techniques to study growth over several weeks (Curtis, 1884). With the advent of U-Th dating in the 1970's, radiometric dates were used to calculate the mean growth rate between dated sections (see review in Ford and Williams, 1989). However, it was not until the work of Dreybrodt (1980, 1981, 1988, 1997; Buhmann and Dreybrodt, 1985a,b) that a theoretical understanding of the rate of stalagmite formation was achieved. These studies, based on the chemical kinetics of the calcite deposition process, allowed a theoretical growth rate to be predicted, based on the chemical and hydrological properties of the drip water feeding the stalagmites and the composition of the cave air. Laboratory testing of the theory demonstrated a good agreement between theoretical and actual growth rate (Buhmann and Dreybrodt, 1985a,b), however field testing for flowstone samples suggested theoretical growth rates overestimated actual growth rates by x2.4 and 4.7 (Baker and Smart, 1995). Several potential factors may cause this discrepancy, including uncertainties in the original Plummer et al (1978) equations upon which the theory is based, seasonal cessation of the water supply, and significant variations in the growth rate determining variables over the time of speleothem deposition. Further studies are required to determine which, if any, of the above factors can explain observed stalagmite growth rate.

This study seeks to provide precise measurements of recent stalagmite growth rate determined from the thickness of individual annual laminae. Laminated speleothems have been reported for over 70 years (Allison, 1926; Orr, 1952; Kirchmayer, 1962; Blanc, 1972; and many others). For example, Orr (1952), counted the laminations on calcite coating nails and found a perfect correlation between the number of laminations and the age in years of the nail deposits. Other demonstrations of the annual nature of laminations have used either ^{14}C (Broecker et al., 1960; Genty and Quinif, 1996), U-Th dating (Baker et al., 1993; Genty and Quinif, 1996), or the history of the site for modern deposits (Genty, 1992, 1993; Genty et al., 1995; Baker and Smart, 1995). Most recently, laminations have come under closer scrutiny as they provide a potential annual record of palaeochronology and palaeoenvironments (Genty, 1992, 1993; Genty and Quinif, 1996; Baker et al., 1993, 1995; Railsback et al., 1994; Shopov et al., 1994).

Testing the validity of theoretical stalagmite growth rate has implications for several areas of karst geology and geomorphology.

Understanding stalagmite growth rates permits an improved understanding of the rate of filling of cave voids by secondary calcite depending on geological and climatic conditions. Several authors have postulated environmental and climatic controls on the different fill percentages and amount of decoration within caves, often within the theoretical underpinnings of climatic geomorphology (Corbel, 1957; Gams, 1965; Ford and Williams, 1989; Sweeting, 1972 1994; Dreybrodt, 1988). More recently, calcium ion concentrations in karst groundwater have been modelled and demonstrated to be predictable from both geological factors (groundwater flow path between the two endmembers of open- and closed-system evolution which lim-

* Author to whom correspondence should be addressed (a.baker@exeter.ac.uk).

its the equilibrium uptake of CO_2) and climatic factors (surface temperature; Drake, 1980, 1983). If calcium ion concentration is the most significant growth rate determining variable, then the theoretical model of Drake (1980, 1983) may be utilised with the growth rate model to provide an improved insight into the rate of development of cave carbonate fills under different environmental conditions.

The growth rate of stalagmites contains a potential palaeoclimate signal as the chemical kinetics of stalagmite growth are dependent on several variables which can be determined by climate and vegetation changes. For example, drip rate may be related to the surface precipitation or soil moisture excess, and the calcium concentration may be dependent on the porosity and permeability of the limestone, as well as the soil moisture, temperature, and thickness conditions as detailed above. Although these examples would suggest that the interpretation of growth rate variations in terms of climate change is fraught with difficulty, it may be possible to integrate growth rate data with other record contained within speleothem calcite ($^{18}0$, ^{13}C, trace elements, pollen, etc.) in order to obtain a multi-proxy record of palaeoenvironmental change.

It has been suggested that there is a relationship between the mineralogy of stalagmites and their growth rate (Genty and Quinif, 1996; Genty et al., 1997). Speleothem crystallography has been underresearched for the last 20 years (notable exceptions include Kendall and Broughton, 1978; Gonzalez et al., 1993; Kendall, 1993; Genty, 1993), but if the growth rate of stalagmites is dependent on the geochemical conditions at the time of deposition, then it may be possible to gain an improved insight into the relationship between geochemistry, growth rate, and calcite crystal structure.

2. THEORETICAL BACKGROUND

Precipitation of calcite from thin stagnant films of water with one surface open to a CO_2-containing atmosphere is a complex process. The precipitation rates are controlled by several quite different processes: (1) surface reactions as described by the rate equations of Plummer et al. (1978) from which the surface precipitation rates can be obtained when the concentrations of the species reacting are known on the surface, (2) the slow reaction of $H^+ + HCO_3^-$ into $H_2O + CO_2$, which is released from the water layer into the atmosphere, and (3) mass transport of the reacting species towards or away from the calcite surface. To obtain precipitation rates under these various processes, which control the rates, one has to solve transport equations which take into consideration these three mechanisms. This has been done by Buhmann and Dreybrodt (1985a,b). In the following we have used their model to calculate precipitation rates as they occur during the growth of speleothems.

To model such rates we assume that a planar calcite surface is covered by a thin layer of water with thickness δ. The free surface of this film is in contact with an atmosphere containing CO_2 with partial pressure, Pco_2. CO_2 is transported within this film to the surface where degassing of CO_2 from the solution occurs, calcite is precipitated, and, therefore, solution calcium concentration decreases as it approaches equilibrium with respect to calcite. Figure 1a shows the precipitation rates as a function of the average concentration of Ca^{2+} in the water film.

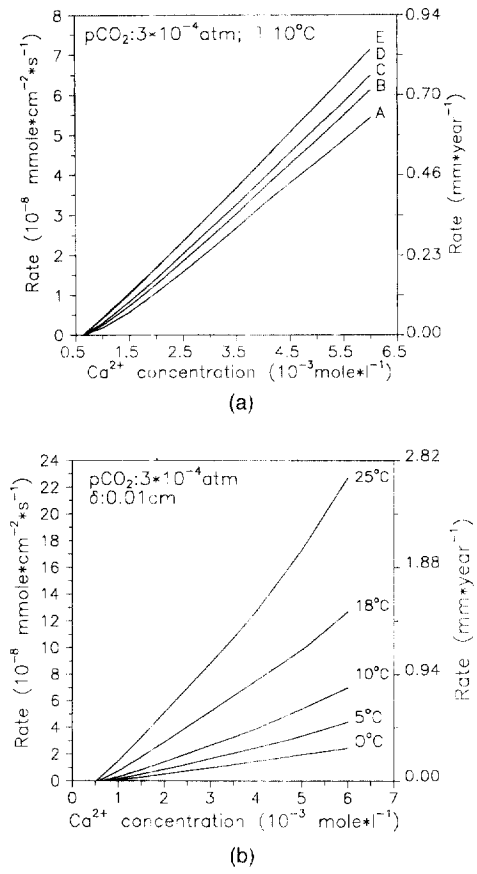

Fig. 1. (a) Precipitation rates at various film thicknesses δ as a function of the average calcium concentrations in the water film (A: δ = 0.005 cm, B: δ = 0.0075 cm, C: δ = 0.01 cm, D: $_{\delta}$0.02 cm; E: $_{\delta}$0.04 cm). (b) Precipitation rates with δ = 0.01 cm for various temperatures denoted at the curves. Pco_2 = 3·10^{-4} atm.

This is the concentration which is measured by chemical analysis. It is different from the concentration at the surface of the mineral. The curves in Fig. 1a depict these rates in mmol cm^{-2} s^{-1} for various thicknesses δ of the supersaturated water film, with $Pco_2 = 3.10^{-4}$ atm at a temperature of 10°C. In the range of 0.04δ0.02 cm (E,D) the rates do not depend on δ. For δ m). In all these cases conversion of HCO_3^- into CO_2 and molecular diffusion are rate limiting (Buhmann and Dreybrodt, 1985a). Figure 1b illustrates precipitation rates for a film with δ = 0.01 cm, $Pco_2 = 3.10^{-4}$ atm at various temperatures. There is a significant increase in the rates with increasing temperature. All the curves in Fig. 1 can be approximated within an error of 10% by a linear relation.

$$R = \alpha(c - c_{eq}) \quad (1)$$

where α is the kinetic constant in cm s^{-1}, c is the calcium concentration in the water film, and c_{eq} is the equilibrium concentration of calcium in mmol cm^{-3} = mol L^{-1}, with respect to calcite. For $Pco_2 = 3 \cdot 10^{-4}$ atm, c_{eq} = 0.475 mmol L^{-1} at 25°C. Within this range the results of the calculation of c_{eq} as function of temperature by use of the program EQUILIBRIUM (Dreybrodt, 1988) can be summarized by the empirical relation

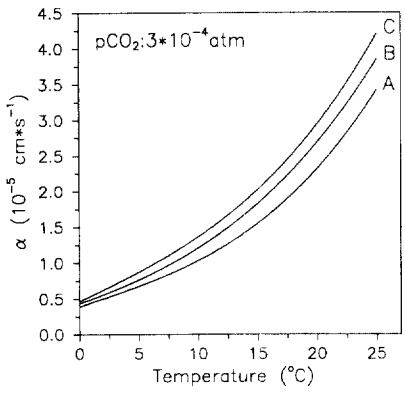

Fig. 2. Values of the kinetic constant α as a function of temperature for film thickness δ = 0.005 cm (A), δ = 0.0075 cm (B), and δ0.01 cm (C).

$$c_{eq} = (-0.01t + 0.72) \cdot 10^{-3} (\text{mol l}^{-1}) \qquad (2)$$

where t is the temperature in °C Fig. 2 shows the values of α as a function of temperature for δ 0.01 cm (C), δ = 0.0075 cm (B), and δ = 0.005 cm (A).

By use of Eqns. 1 and 2 and Fig. 2 one can estimate rates for the Ca concentration above $1.5.10^{-3}$ mol L^{-1} to a satisfying accuracy. Close to equilibrium inhibition processes might be present, which may reduce the rates significantly (Dreybrodt et al., 1997).

These data can now be used to estimate growth ratetration decreases exponentially in time with a time constant $\tau = \delta / \alpha$. The average molecular accumulation rate between two drops falling onto it at a time interval T has been shown (Dreybrodt and Franke, 1987; Dreybrodt, 1988) as

$$R_{acc} = (c - c_{eq})\ \delta / T(1 - \exp(T/\tau))\ \text{mmol cm}^{-2}\,\text{s} \qquad (3)$$

If $T \leq 0.2\delta/\alpha$, R_{acc} can be estimated from Eqn. 1 with an accuracy of 10%. For δ = 0.005 cm and a temperature of 10°C one can read from Fig. 1 that $\alpha = 10^{-5}$cm s^{-1}. Thus reliable growth rates can be estimated for T smaller than 100 s. Otherwise Eqn. 3 has to be employed to calculate R_{acc}.

So far a standard atmospheric Pco_2 of $3{\cdot}10^{-4}$ atm has been assumed. Caves, however, can exhibit much higher values (Ek and Gewelt, 1985). Therefore, we have calculated deposition rates for various Pco_2. This is visualized by Fig. 3 for a film with δ = 0.005 cm and 10°C for various Pco_2 from $3{\cdot}10^{-4}$ up to $5{\cdot}10^{-3}$ atm. From Fig. 3 one reads that α remains unchanged. Therefore, Eqn. 1 remains valid with the α obtained from Fig. 2, provided c_{eq} is changed according to the higher Pco_2. For Ca concentrations above 2.10^{-3} mol L^{-1} only small changes of the rates occur for $Pco_2 < 2{\cdot}10^{-3}$ atm. When foreign ions are present in the solution, it is also possible to give satisfactory estimations for precipitation rates. Dreybrodt and Buhmann (1987) have shown that in this case α, which depends only on temperature and film thickness, remains unchanged and Eqn. 1 can be used if c_{eq} is the concentration of equilibrium with respect to calcite in the corresponding solu-

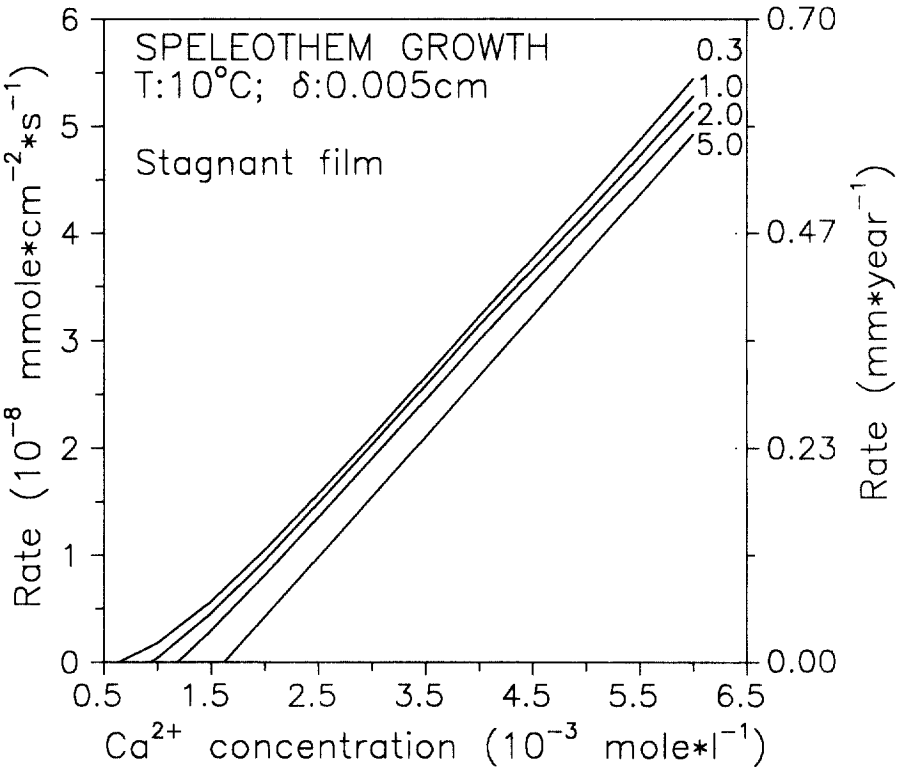

Fig. 3. Precipitation rates as a function of average calcium concentration for δ = 0.005 cm, T = 10°C for various Pco_2 partial pressures, denoted by the numbers in 10^{-3} atm.

tion. c_{eq} can be obtained by use of programs, such as EQUILIBRIUM1 (Dreybrodt 1988). Although this was realized only for undersaturated solutions (Dreybrodt and Buhmann, 1987), it also holds for precipitation, since the mechanisms involved are identical.

The rates are converted from mmol $cm^{-2}s^{-1}$ into molecular accumulation rate in cm/yr by the factor $3.145 \cdot 10^6/\rho$, where ρ is the density of limestone in g cm^{-3}. With $\rho = 2.7$ g cm^{-3} this factor becomes $1.17 \cdot 10^6$ cm^3 s (mmol yr^{-1}). This is correct when the calcite is deposited in such a way that it is compact. However, speleothem calcite is not always the density of pure calcite; we have measured a 10% porosity in white calcite fabrics of stalagmites (Genty et al., 1997). Porosity is due to a weaker crystalline coalescence which is still not very well understood (Kendall and Broughton, 1978). Because the same concentration of molecular accumulation rate determining variables can produce different stalagmite growth rates depending on porosity, we have to correct the model results. The porosity factor can be calculated by measuring the weight and volume of calcite slabs extracted from stalagmite samples. Given that the mean growth rate $R_{act} = R_{acc} + R_v$, where R_{acc} is the growth rate assuming a volume comprising 100% calcite (Eqn. 3), and R_v is the apparent growth rate from the voids within the stalagmite calcite, then:

$$R_{act} = R_{acc}\,(1 + \phi) \tag{4}$$

where ϕ is the porosity. Since porosities are small, however, in the order of about $10 \pm 5\%$, this is not a significant correction in view of the many other uncertainties arising during the growth of speleothems, such as changing climate, different water supply, and so on.

So far we have assumed the water layers as stagnant. If there is flow directed outwards from the central dripping point this will not affect the deposition rates. Flow in any case will be laminar. As has been shown by Buhmann and Dreybrodt (1985a,b), deposition from a laminar flowing film with a given concentration is the same as that from a stagnant film.

3. SITE DESCRIPTIONS AND ANALYTICAL METHODS

3.1. Site Descriptions

In order to adequately test theoretical stalagmite growth rate, cave sites need to fulfil the following criteria. (1) Sites must contain actively forming laminated samples, in which the laminations can be demonstrated to be annual, to give the highest resolution and best constrained records of growth rate. The stalagmites must also be of the candlestick type in order to have the simplest morphology with which to assess the growth rate theory. (2) The sites need to be such that a wide range of variability in the growth rate determining variables can be sampled. (3) The sites must have remained undisturbed in terms of overlying vegetation change so that one can be confident that the growth rate determining variables measured today reflect those of the time of stalagmite deposition. Three sites were chosen which fitted the above criteria (Fig. 4)

3.1.1. Brown's Folly Mine, Bathford, Wiltshire, England

This sample site, situated in the oolitic limestone of the Jurassic, was formed by building stone mining activity between 1836 and 1886 (Price, 1985). Since its abandonment, its entrances were closed for c. 100 years until reopened by cavers in the 1970s. The overlying vegetation is secondary woodland which is managed as part of a local nature reserve and has not changed for the last 100 years. The mine is highly decorated with juvenile candlestick-type speleothem formations, samples chosen for this study originate from a part of the mine signed-off in 1836 (M. Leyshon, pers. commun.), which provides a crude indication of the minimum growth rate of the samples. Many of the stalagmite samples are laminated.

3.1.2. Grotte de Villars, Dordogne, France

This sample site, situated in the Jurassic limestone, is a well decorated showcave, overlain by secondary woodland which has remained undisturbed over the last 100 years. The cave contains a large quantity of pre-Holocene fill of finely laminated or nonlaminated clays and silts, upon which Holocene speleothem deposition has occurred. Many of these samples were of candlestick-type and have fallen and broken as the clay and mud banks have subsided over time and were thus available for scientific analysis. The majority of stalagmites are laminated.

3.1.3. Godarville Tunnel, Godarville, Belgium

This sample site is an abandoned tunnel built in 1885 to permit the passage of a canal from Mons and Charleroi. The tunnel is constructed in clays and calcareous sands of the Ypresian (Lower Eocene) and was abandoned and sealed in the 1960s when a surface cutting was constructed for the canal. Speleothem formation, including many juvenile candlestick-type stalagmites, commenced after this date, and several studies have demonstrated annual laminations within them (Genty, 1992, 1993; Genty and Quinif, 1996).

3.2. Measurement of Laminae Thickness

Two standard techniques are available to determine the thickness, and hence growth rate, of annual laminations within speleothems, depending on whether the laminations are visible under UV or visible light. Under visible light, for samples from France and Belgium, visible laminae were observed using digital image processing at the Universite de Paris-Sud. The samples were illuminated using a 9W neon light source, and the reflected light visible in the 400–1000 nm range detected using a black and white CCD video camera connected to a computer. Individual laminations were quantified by grey levels from 0 to 255 over two dimensions and laminae thickness measured from grey level inflection points. Laminations are also observable under UV light; this technique is particularly useful when growth rate is too slow to allow observation under visible light and also where there are high concentrations of mineral matter which obscures the annual signal from organic matter variations (Genty et al., 1997). For the lower growth rate site of Brown's Folly Mine, a Zeiss Axiotech microscope, with a mercury light source to excite luminescence, was utilised. Images were captured on Ilford FP/5 film, and the resulting images scanned, image processed, and laminae thickness measured from luminescence inflection points. The sampling locations for stalagmite samples in Brown's Folly Mine, Grotte de Villars, and Godarville Tunnel are presented in Fig. 4.

3.3. Measurement of Growth Rate Determining Variables

At all three sites the drip waters were predominantly supersaturated with respect to calcite, and those waters which were forming candlestick-type stalagmites were collected over the hydrological years in either 1995–1996 or 1996–1997 to determine the natural variability of the growth rate determining variables (the concentration of Ca ions in the drip water (Ca^{2+}), water temperature (T), and the drip rate of water onto the sample Q). Ca^{2+} was determined from 125 mL water samples collected in glass bottles, glass stoppered, filled to the top, and subsequently filtered and preserved with HNO_3 before analysis using an AAS. Temperature was recorded using hand-held electronic thermometers accurate to 0.1 °C, and the drip rate by measuring the average time between drips for between five and ten drips. In addition, samples were collected from many different points in both Brown's Folly Mine and Grotte de Villars so that spatial variability could be compared to temporal variability. In order to be certain that no degassing had occurred, and to demonstrate both a complete ion balance for the drip water chemistry as well as calcite saturation, full ion chemistry was performed when practicable (e.g., under conditions of high discharge). pH was performed in situ, and HCO_3^- by titration with 0.1 N HCl immediately after sample removal from the cave environment. Ion

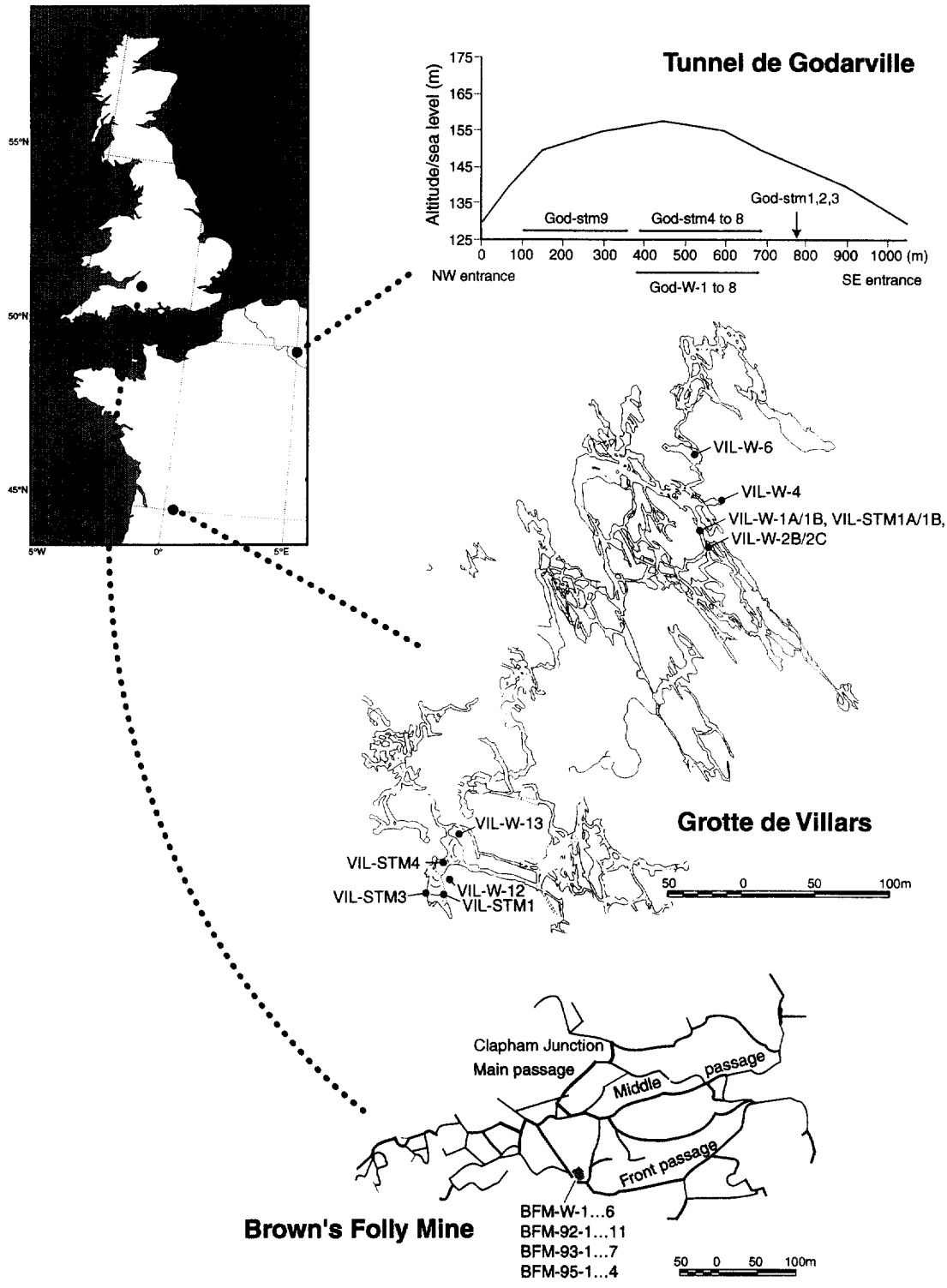

Fig. 4. Stalagmite and drip water sampling locations for Brown's Folly Mine, Grotte de Villars, and Godarville Tunnel.

balance was calculated using PC WatEqf (Plummer et al., 1976). Where possible, water samples were collected which were directly related to a stalagmite which had been sampled (four sites in Brown's Folly and two sites in Grotte de Villars). However, this was not always possible (e.g., where stalagmite samples were those which had fallen from their active deposition location), and, therefore, it has to be assumed that the spatial variability of water chemistry data was typical of all drips generating speleothem growth. Water sampling locations for the three sites are presented in Fig. 4.

Pco_2 measurements were made using a Draeger pump with CO_2 tubes calibrated to the range 0.01–3.0 ppm. Point samples were taken, as Ek and Gewelt (1985) demonstrated that seasonal variability is of the order of

Table 1. Vertical height of stalagmite samples from Brown's Folly Mine calculated from annual laminae thickness and from actual sample vertical height

Sample ID	Vertical Height of laminated sections (mm)	Number of Laminations (n)	Mean growth rate determined from laminae thickness (mm)	Stalagmite Vertical height (mm)	Mean growth rate determined from vertical height (mm yr^{-1})
BFM-92-1	no laminae	-	-	2.5	0.016
BFM-92-2	no laminae	-	-	4.5	0.028
BFM-92-3	no laminae	-	-	3.7	0.023
BFM-92-4	no laminae	-	-	5.0	0.031
BFM-92-5	0.90	9	0.10±0.03	3.6	0.023
BFM-92-6	1.37	6	0.23±0.12	10.2	0.064
BFM-92-7	1.40	10	0.14±0.02	24.4	0.153
BFM-92-8	0.64	8	0.08±0.02	12.5	0.078
BFM-92-9	no laminae	-	-	22.7	0.017
BFM-92-10	2.12	13	0.16±0.05	11.2	0.070
BFM-92-11	1.35	15	0.09±0.03	15.4	0.096
BFM-93-1	0.55	5	0.11±0.04	21.3	0.133
BFM-93-2	1.05	21	0.05±0.02	11.5	0.072
BFM-93-3	no laminae	-	-	18.3	0.114
BFM-93-4	no laminae	-	-	13.3	0.083
BFM-93-5	no laminae	-	-	15.4	0.096
BFM-93-6	0.81	9	0.09±0.03	13.2	0.083
BFM-93-7	no laminae	-	-	16.4	0.103
BFM-95-1	1.11	14	0.08±0.04	12.0	0.075
BFM-95-2	no laminae	-	-	4.0	0.025
BFM-95-3	0.37	5	0.07±0.01	11.5	0.072
BFM-95-4	2.20	17	0.13±0.05	25.1	0.157
BFM-95-5	2.66	19	0.14±0.05	25.1	0.157
Mean			0.12±0.05		0.077±0.044

Porosity of BFM-95-3 8±2%, BFM-92-7 6±1%

100%, which is not significant compared to the spatial variability observed in cave environments. The thickness of the water film on the stalagmite cap was assumed to be 0.045 ± 0.019 mm, the mean of seventy-two measurements of water film thickness taken in the cave environment using a vernier spherometer (Baker, 1993), similar to measurements of the order of 0.1 mm calculated from the weight change of filter papers which had absorbed the water on the stalagmite cap (Dreybrodt, 1988). It is also assumed that, as sites were chosen with unchanged vegetation cover, the water samples collected are representative of those over the time of stalagmite deposition (the last 30–100 years).

4. RESULTS

4.1. Growth Rates Determined from Stalagmite Annual Laminae Thickness

4.1.1. Confirmation of annual nature of laminations

Although the stalagmites at the three sites contained laminations, there can be no prior assumption made that these

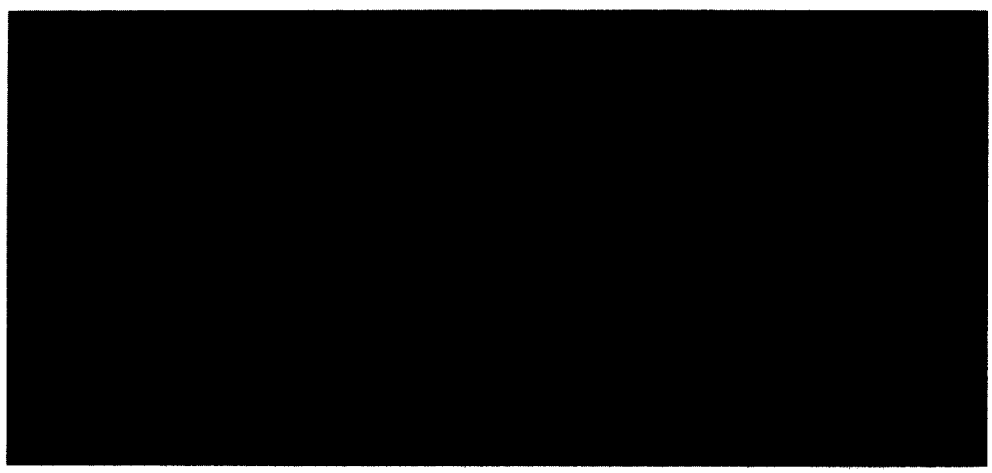

Fig. 5. Laminations within BFM-93-2 at a position 1 mm from the base. Image taken using UV mercury lamp excitation and x25 magnification. Note the discontinuous nature of the laminations.

laminae are annual. Thus the age of the cave, mine, or artificial tunnel was used to provide a less precise estimate of the annual nature of laminations, as the maximum age of the speleothems is constrained by the age of the void in which they are forming, as previously reported for the Godarville Tunnel (Genty, 1992; Genty and Quinif, 1996). Where laminations are not continuous, the total vertical height of speleothem deposited over the known maximum time period available for deposition can be utilised to calculate a minimum growth rate. If the growth rate determined from lamination counting is statistically similar, then this suggests the laminae are annual, whereas if more laminae are present compared to that possible on an annual basis, then they have to be subannual.

For Brown's Folly Mine the mean and standard deviation growth rate was calculated from total sample vertical height. All deposition has to be in the last 160 years, since the time of last working in the relevant section of mine. This growth rate was compared to the laminae thickness, assuming that the laminae are annual. The results are presented in Table 1. Mean growth rate predicted from sample vertical height averaged over the 160 years equalled 0.077 ± 0.044 mm yr^{-1} (th rate as sample deposition could have been discontinuous over this time period or have commenced some time after mine abandonment. Absolute growth rate calculated assuming annual laminae deposition and determined from multiple laminae within each stalagmite sample equalled 0.11 ± 0.05 mm yr^{-1} (n = 13). Within-sample variability of laminae thickness was high, with a coefficient of variation of 28 ± 10%, and laminations were not continuously preserved within any of the samples (Fig. 5). The good agreement between the predicted and actual mean growth rates confirms that the majority of laminae deposition is annual. When both growth rate measurements are plotted against each other, it is apparent that there is a good agreement for ten out of the thirteen samples (Fig. 6). For the other three, annual growth rate from laminae is two to four times greater than growth rate averaged over 160 years. This may reflect cessation of stalagmite deposition, either over several years (for example, speleothem deposition need not commence immediately after mine abandonment) or subannually (for example, due to a summer drip cessation).

To confirm recent stalagmite deposition in the Grotte de Villars, all stalagmite samples had active drip sources when collected. In addition, the stalagmite associated with the water source Vil-W-1a had a varnish marker placed on its surface in 1995 and, upon sectioning one year later, revealed a growth rate equal to other samples at the site. Finally, ^{14}C analyses were undertaken on Vil-stm1. This stalagmite demonstrated very clear and continuous laminations (Fig. 7), and ^{14}C was measured at the top and bottom of the laminae sequence. The difference in ^{14}C (assuming a constant dead-carbon percentage over time) demonstrated that 210 ± 120 years had elapsed, statistically equal to the number of laminations (n = 198). For other samples at the site we have assumed that laminations are annual because of their regularity and similarity with demonstrated annual laminations from Vil-stm1 (Fig. 7) and elsewhere.

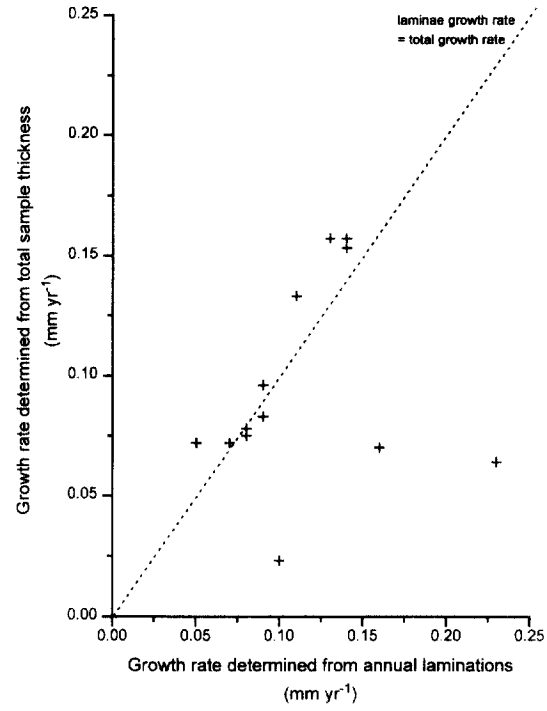

Fig. 6. Comparison of growth rates determined from annual lamination counting with those determined from total sample deposition over the last 160 years at Brown's Folly Mine. The dashed line is the assumed relationship if laminae growth rate is equal to the average growth rate for the total time of sample deposition. The three outliers are BFM-92-5, BFM-92-6, and BFM-92-10.

4.1.2. Growth rates determined from annual laminae thickness

Brown's Folly Mine. Growth rates calculated both from the total sample vertical height since the date of mine opening, as well as from direct measurements of laminae thickness in UV light, are presented in Table 1 and demonstrate no difference between the mean and standard deviation growth rate for the samples; 0.11 ± 0.05 mm yr^{-1} (1σ; n = 13) for laminae thickness measurements and 0.077 ± 0.044 mm yr^{-1} (1σ; n=23) from total sample vertical height. As discussed above the former is likely to be maximal and the latter a minima. Therefore, mean growth rates at the site can be expected to be observed in the range 0.04–0.16 mm yr^{-1}, although occasionally growth rates may exceed this to a maximum of ~0.2 mm yr^{-1}.

Grotte de Villars. The growth rates for stalagmites from the Grotte de Villars, based on the thickness of annual laminations, are presented in Table 2. Mean growth rate from the site was measured to be 0.55 ± 0.35 mm yr^{-1} (n = 5).

Godarville. Growth rates for the Godarville Tunnel samples were calculated using the thickness of annual laminae deposited since the time of stalagmite deposition commencement (1960). The results are presented in Table 3; mean growth rate from the site was determined to be 0.89 ± 0.38 mm yr^{-1} (n = 9).

To investigate the importance of porosity on the growth rate of the stalagmites, several samples were measured by calculat-

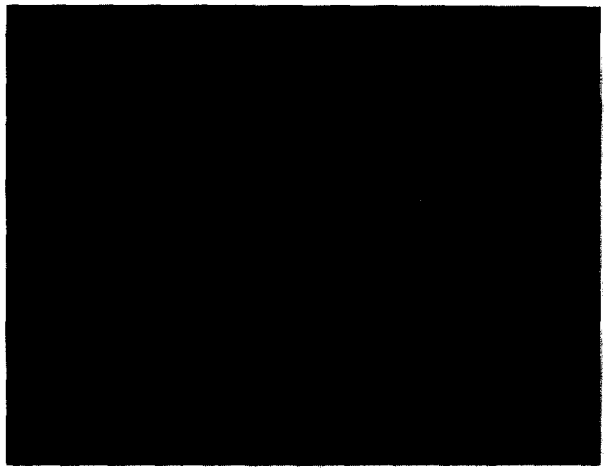

Fig. 7. Laminations within Vil-stm1 for the top 100 mm of calcite as observed under visible light.

ing the weight and volume of some calcite slabs extracted from the stalagmites. Results are presented in Tables 1 and 2. It is apparent that porous stalagmite calcite will mean that the true growth rate is underestimated by ~10% by the theoretical molecular accumulation rate alone, which does not incorporate porosity as a factor.

4.2. Measurement of growth rate determining variables

Brown's Folly Mine data were collected over the 1996–1997 hydrological year for seven sample sites; results are presented in Table 3a. During the sampling programme, it was apparent that intra-annual variability of major ion concentration at a given site was not as significant as spatial variability within the mine. Thus additional point water samples were collected for geochemical analysis, and these data are presented in Table 3b. Mean Ca ion concentrations for the entire mine equalled 2.20 ± 0.32 mmol L^{-1} (n = 17; C.V. = 15%); the intersample variability of Ca ion concentration is similar to the within sample variability over the hydrological year (C.V. = 13.0 ± 4.8%; n = 4).

Table 3a demonstrates that, for the stalagmites sampled, variability in drip discharge onto the stalagmites was greater than the variability of dripwater chemistry. Some seasonal hydrological variations were also observed; in particular it can be noted that two of the four sites monitored experienced a cessation of water flow (BFM-W-4 was dry in September and BFM-W-1 was only wet under unusually wet spells in November to March) and thus would not experience calcite deposition over this study period. When discharge did occur, the range was from 0.001 to 1 drips s^{-1}; this range of values will be used as input to the model. Pco_2 data were collected between October 1996 and August 1997; results demonstrated no seasonal variations with Pco_2 in the range 0.0035–0.0040 atm at the stalagmite sampling locations. Air and water temperature measurements were collected throughout the seasonal cycle. Water temperatures averaged 9.9±0.1°C (n=10); air temperatures averaged 10.0 ± 0.4°C (n = 12); no seasonal variability was observed within either data set.

Grotte de Villars data were collected over the 1995–1996 hydrological year for four sample sites representing a wide range of drip discharges. The results are shown in Table 4a. During the sampling programme, it was apparent that intra-annual variability of major ion concentration was not as significant as spatial variability within the site. Thus additional point water samples were collected for geochemical analysis and are presented in Table 4b. Mean Ca concentration for the site was 3.29 ± 0.42 mmol L^{-1} (n = 9; C.V. = 13%), with spatial variability slightly greater than variability over the hydrological year (C.V. = 6.2 ± 2.1%).

Intra-annual variability of discharge varied between 29 and 138% for individual samples, with a range of between 0.0025 and 1 drips s^{-1}. For data input into the growth rate model, the latter discharge range can be considered representative of current conditions at the site. Water and air

Table 2. Growth rate of stalagmite samples from Grotte de Villars and Godarville Tunnel based on visible laminae thickness

Sample ID	Number of Laminae	Mean Visible Laminae Thickness (mm)	Porosity (%)
Vil-stm1a	11	1.00±0.10	n.d.
Vil-stm1b	13	0.86±0.10	n.d.
Vil-stm1	17	0.55±0.11	10.7±0.5
Vil-stm3	10	0.19±0.02	n.d.
Vil-stm4	7	0.21±0.04	n.d.
Mean		0.55±0.35	
God-stm1	40	0.72	14.7
God-stm2	42	0.94	12.8
God-stm3	40	0.47	3.9
God-stm4	39	0.68	10.9
God-stm5	32	1.44±0.41	14.9
God-stm6	44	0.94	n.d.
God-stm7	44	0.71	n.d.
God-stm8	44	0.59	11.1
God-stm9	42	1.56	n.d.
Mean	0.89±0.38	11.7±3.5	

Table 3. Geochemical data for Brown's Folly Mine for the 1996-1997 hydrological year.

Sample I.D.	n	Q (drips/s)	pH	Ca^{2+} (mmol l^{-1})	Mg^{2+} (mmol l^{-1})	Na^{+} (mmol l^{-1})	Cl^{-} (mmol l^{-1})	SO_4^{2-} (mmol l^{-1})	HCO_3^{-} (mmol l^{-1})	Ion B. (%)	S.I. (calcite)
(a) Seasonal data											
BFM-W-1	20	1.27±2.13*	8.12±0.24	2.23±0.38	0.28±0.05	0.15±0.01	0.52±0.10	0.12±0.02	3.30±0.20	9±3	0.86±0.06
BFM-W-2	20	2.64±3.21	7.77±0.26	2.48±0.15	0.32±0.09	0.15±0.01	0.58±0.23	0.15±0.18	4.02±0.40	7±4	0.44±0.22
BFM-W-3	20	1.13±1.48*	7.89±0.22	2.34±0.43	0.34±0.16	0.15±0.01	0.48±0.08	0.11±0.04	3.93±0.24	8±3	0.74±0.19
BFM-W-4	15	0.13±0.22	7.79±0.42	2.39±0.26	0.44±0.18	0.15±0.02	1.04±0.68	0.14±0.09	4.02±0.03	5±4	0.84±0.16
(b) Point data											
BFM-W-3a		0.33	7.75	2.23	0.61	0.16	0.36	0.09	nd	nd	nd
BFM-W-5		0.016	8.06	2.03	0.65	0.13	0.38	0.09	3.00	nd	nd
BFM-W-6		0.66	nd	2.2	0.12	0.16	0.33	0.09	nd	nd	nd
BFM-W-7		0.007	7.85	2.38	0.24	0.17	0.45	0.11	nd	nd	nd
BFM-W-8		7.1	8.02	2.48	0.14	0.08	0.47	0.09	4.90	0.2	0.779
BFM-W-9		0.014	7.76	1.85	0.21	0.15	0.49	0.10	nd	nd	nd
BFM-W-10		10	nd	2.43	0.27	0.94	0.84	0.46	nd	nd	nd
BFM-W-11		0.23	nd	1.60	0.08	0.34	0.45	0.15	nd	nd	nd
BFM-W-12		0.013	8.36	2.38	0.22	0.13	0.78	0.12	nd	nd	nd
BFM-W-13		0.04	7.50	2.60	0.26	0.14	0.39	0.07	nd	nd	nd
BFM-W-14		0.03	7.80	2.35	0.21	0.13	0.53	0.09	nd	nd	nd
BFM-W-15		0.008	8.07	2.00	0.21	0.15	0.28	0.09	nd	nd	nd
BFM-W-16		0.02	7.83	1.40	0.19	0.14	0.38	0.06	nd	nd	nd

nd = no data. * = seasonally dry

temperature readings were undertaken at various points in the cave system throughout the year; no significant difference was determined (water: 10.9 ± 0.1, n = 4; air: 11.2 ± 0.5, n = 30). Pco_2 measurements were also taken at the sampling locations within the cave between November 1996 and May 1997 and ranged from 0.008 to 0.013 atm (n = 6).

Godarville Tunnel data were collected over the 1996–1997 hydrological year, with less frequent sampling intervals than the other two sample sites due to its remoteness from the authors. The results are presented in Table 4a. Pco_2 concentrations equalled 0.0035 atm (Verheyden, unpubl. data), and water temperatures equalled that of the air temperature of the site (9.8 ± 0.4 °C (n = 4) and 9.7 ± 0.5 °C

Table 4. Geochemical data for Grotte de Villars and Godarville Tunnel. Data for Grotte de Villars is from the 1995–1996 hydrological year, data for Godarville Tunnel is from the 1996–1997 hydrological year.

Sample I.D.	n	Q (drips/s)	pH	Ca^{2+} (mmol l^{-1})	Mg^{2+} (mmol l^{-1})	Na^{+} (mmol l^{-1})	Cl^{-} (mmol l^{-1})	SO_4^{2-} (mmol l^{-1})	HCO_3^{-} (mmol l^{-1})	Ion B. (%)	S.I. (calcite)
(a) Seasonal data											
VIL-W-1a	7	0.08±0.02	7.56±0.21	3.25±0.15	0.08±0.01	0.27±0.20	0.20±0.04	0.05±0.07	7.01±0.01	8±6	0.39±0.33
VIL-W-1b	7	0.25±0.12	7.55±0.25	3.22±0.18	0.08±0.01	0.21±0.04	0.17±0.02	0.04±0.07	7.21±0.35	12±6	0.52±0.19
VIL-W-2b	4	0.13±0.18*	7.37±0.20	3.47±0.17	0.06±0.01	0.18±0.09	0.14±0.03	0.07±0.06	6.97	1	0.44
VIL-W-4	5	0.42±0.56	7.51±0.21	3.05±0.30	0.06±0.01	0.40±0.08	0.26±0.15	0.03±0.03	7.21±0.02	8±5	0.51±0.19
God-w-1	4	1.07±0.15	7.27±0.28	5.28±0.95	0.44±0.15	0.51±0.13	0.85±0.44	1.16±0.45	4.53±1.44	23±6	0.36±0.24
God-w-3	2	1.37	nd	3.35±6.95	0.40±0.73	0.40±0.46	0.78±0.50	0.90±2.93	n.d.	n.d.	n.d.
God-w-4	4	0.10±0.28	7.76±0.21	4.56±0.63	0.27±0.03	0.46±0.12	0.70±0.09	0.82±0.22	4.74±1.72	20±8.	0.95±0.28
God-w-6	3	>5.0	7.44±0.09	3.63±0.43	0.39±0.01	0.41±0.08	0.79±0.07	0.44±0.05	4.18±0.86	18±4	0.27±0.13
God-w-7	4	0.37±0.74	7.78±0.26	7.79±2.32	0.52±0.04	0.37±0.16	0.67±0.04	2.26±1.16	3.99±1.41	23±7	0.81±0.20
God-w-8	3	2.20±4.09	7.18±0.33	8.46±1.84	0.77±0.03	0.53±0.09	1.20±0.01	1.97±1.74	6.88±1.73	12±60	0.54±0.25
(b) Point data											
VIL-W-2c		0.043	7.56	3.23	0.06	0.2	0.27	n.d	n.d.	n.d.	n.d.
VIL-W-6		0.200	7.56	3.70	0.06	0.38	0.32	n.d	n.d.	n.d.	n.d.
VIL-W-12		1.000	7.44	3.23	0.13	0.24	0.12	n.d	n.d.	n.d.	n.d.
VIL-W-13		0.200	7.35	4.05	0.15	0.34	0.30	n.d	n.d.	n.d.	n.d.
VIL-W-10		0.017	nd	2.45	0.03	0.14	0.17	n.d	n.d.	n.d.	n.d.

n.d. = no data. * = seasonally dry

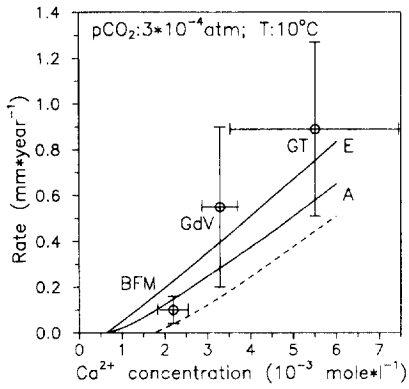

Fig. 8. Comparison between molecular accumulation rates observed and the theoretical prediction The full lines A and E refer to $\delta = 0.005$ cm and $\delta = 0.2$ cm respectively (cf. also Fig. 1a). The dashed line corresponds to the full line A but shifted to a new equilibrium concentration due to the presence of $CaSO_4$. BFM = Browns Folly Mine, GdV = Grotte de Villars, GT = Godarville Tunnel. The results are not corrected for a 10% porosity of calcite.

(n = 3), respectively). Mean Ca concentration at the site equalled 5.51 ± 1.96 mmol L^{-1} (n = 6) and the drip rate onto the samples between 0.1 - 1 drips s^{-1}; this range of discharge was used as a model input.

5. DISCUSSION

Figure 8 demonstrates the relationship between observed and calculated values assuming a temperature of 10°C, a Pco_2 of $3 \cdot 10^{-4}$ atm, and $\delta = 0.005$ cm. We have compared the average growth rates from the three caves to the theoretical molecular accumulation rate predictions. The standard deviation 1σ is also illustrated for both growth rates and Ca concentration. In view of the many uncertainties during growth of the samples, this can be regarded as satisfactory agreement for the data of Brown's Folly Mine and Grotte de Villars.

Some comment is needed for the growth rates from Godarville Tunnel. In contrast to the two other sites the drip water of this site contains elevated concentrations of SO_4^{2-} (1.19 ± 0.77 mmol L^{-1}). It is reasonable to assume that this is due to dissolution of gypsum or anhydrite. This causes a common-ion effect (Atkinson, 1983), as the equilibrium concentration with respect to calcite rises due to the Ca which comes from dissolution of $CaSO_4$. A crude estimation of this equilibrium concentration $c_{eq}SO_4$ is obtained by adding the additional amount of Ca, equal to the concentration $[SO_4^{2-}]$ to the c^0_{eq} of a pure bicarbonate solution (Buhmann and Dreybrodt, 1987). Thus $(c - c_{eq}SO_4^{2-}) \sim c - (c^0_{eq} + [SO_4^{2-}])$. Therefore, the theoretical curve is shifted by about 1 mmol L^{-1} to a higher equilibrium value (dashed curve and the data have to be compared to this curve (cf. theoretical section). In contrast to the other sites, the observed rates are still too high by a factor of two, although there is agreement within 2σ standard deviation. The elevated concentration of Cl^- in the dripwater of Godarville also could cause a shift in the Ca equilibrium concentration due to the ionic-strength effect (Buhmann and Dreybrodt, 1987). However a Cl^- concentration of 5 mmol L^{-1} would cause a shift of about 0.1 mmol L^{-1} and, therefore, does not affect the rates to a significant extent.

It is apparent from Fig. 8 that stalagmite growth rate does appear to be most sensitive to variations in Ca ion concentrations. Growth rate theory suggests that drip rate is also an important variable, and this relationship was investigated for four laminated stalagmites from Brown's Folly Mine where annual drip rate data are available. Correlation analysis suggests a statistically insignificant relationship (r = 0.29, n = 4); however, only two samples were hydrologically active for all of the annual field cycle and when the number of months of water availability was correlated against growth rate a better relationship was observed (n = 4; r = 0.99). Although this statistic must be treated with caution, as the sample size is small, there is no thorough demonstration that the variables are linearly correlated, and that annual field data is being compared to growth rates averaged over the last 160 years; this result suggests that water supply constraints may be worthy of further investigation as a control on calcite deposition, as undertaken in Godarville Tunnel stalagmites God-stm5 and God-stm10 by Genty and Quinif (1996).

The geochemical data from Brown's Folly Mine and Grotte de Villars both demonstrate significant variability in the growth rate determining variables, especially drip rate and Ca ion concentrations. Both spatial and temporal variations occur; over the annual time scale it is apparent that spatial variability in Ca ion concentration is greater than temporal variations. However, when the variability in the growth rate over the whole of the deposition period is considered, then it is apparent that significant temporal variations occur. This suggests that geochemical variations measured over one annual cycle may not be enough to predict long-term variations in growth rate determining variables, in particular variations in dripwater Ca concentration.

6. CONCLUSIONS

The results demonstrate that the Dreybrodt theory does adequately predict actual growth rates over the range of conditions in the cave environment tested here to within 2 standard deviations. However, the sensitivity of stalagmite growth rate to variations in drip water calcium concentration makes palaeoclimatic interpretations difficult, as this factor depends on the soil temperature, soil moisture conditions, seasonality of surface climate, soil depth, vegetation type, bedrock purity, porosity and permeability, and the evolution path of the groundwater between open- and closed-system endmembers. The Ca ion concentrations observed here agree very well with the total range of predicted Ca concentrations of groundwater (from 4.5 mmol L^{-1} for open-system evolution to 1.8 mmol L^{-1} for closed-system evolution) for a mean annual temperature of 10–11°C (Drake, 1980, 1983) and suggests that changes in Ca concentration over time may reflect changes in groundwater flow path as well as changes in palaeoclimate. In addition, a possible relationship between water supply and growth rate is demonstrated here, a similar result to that observed for some stalagmites by Genty and Quinif (1996). However, the link between stalagmite drip water supply and climatic vari-

ables such as surface precipitation or soil moisture excess is complex, with both nonlinear effects, as well as underflow and overflow types of behaviour, for some stalagmites (Baker et al., 1997). The high variability of growth rates between samples within individual sites suggest that multiple samples are required and that individual samples must not be used to infer site geochemical or palaeoclimatic conditions.

The results presented here demonstrate that the kinetic theory of stalagmite growth rate does accurately predict observed growth rates within 2 standard deviations. Future research needs to look at variations in annual growth rates for multiple samples over long (10^2-10^4 yr) time scales in comparison with other proxy records contained within the stalagmite calcite. In addition, structural variations within laminae, e.g., ratio of light to dark or high to low luminescence, for bundled samples over smoothed years of data may provide insight into the hydrological controls on stalagmite growth. This is the focus of current research.

Acknowledgments—University of Exeter Research Fund to AB, NERC funding, and a Royal Society equipment grant to AB/WLB, financial support of the Deutsche Forschungsgemeinschaft to WD. Andrew Teed and Barry Phillips at Exeter for photography. Jo Small, Steve Quantrill, Chris Proctor, and Mike Leyshon for field assistance in UK, Sophie Verheyden for field assistance in Belgium. Access to BFM was made possible by The Wildlife Trust for North Somerset, South Gloucestershire, Bristol and Bath. Access and sampling within GdV was courtesy of Th. Baritaud and H. Versaveau. Access to GT was courtesy of Y. Quinif and M. Dambrain. GdV map is from P. Vidal and Th. Baritaud (Speleo Club de Perigeux).

REFERENCES

Allison V. C. (1926) The antiquity of the deposit in Jacob's Cavern. *Amer. Mus. Nat. Hist. Anthropol. Pap.* **19**, 294–325.

Atkinson T. C. (1983) Growth mechanisms of speleothems in Castleguard Cave, Colombia Icefield, Alberta, Canada. *Arctic Alpine Res.* **15**, 523–536.

Baker A. (1993) *Speleothem growth rate and palaeoclimate.* Ph.D. Thesis, Univ. Bristol.

Baker A. and Smart P. L. (1995) Recent flowstone growth rates: Field measurements in comparison to theoretical predictions. *Chem. Geol.* 122, 121–128.

Baker A., Smart P. L., Edwards R. L., and Richards D. A. (1993) Annual growth banding in a cave stalagmite. *Nature* **364**, 518–520.

Baker A., Smart P. L., Barnes W. L., Edwards R. L., and Farrant A. R. (1995) The Hekla 3 volcanic eruption recorded in a Scottish speleothem. *The Holocene* 5, 336–342.

Baskaran M. and Ilcliffe T. M. (1993) Age determination of recent cave deposits using excess Pb-210 - A new technique. *Geophys. Res. Lett.* 20, 603–606.

Blanc J. J. (1972) Recherches sur les planchers stalagmitiques et les remplissages anciens des grottes du massif de Marseillevyre. *Mus. Anthropol. Prehist. Monaco Bull.* **35**, 5–35.

Broecker W. S., Olson E. A., and Orr P. C. (1960) Radiocarbon measurements and annual rings in cave formations. *Nature* **185**, 93–94.

Buhmann D. and Dreybdrodt W. (1985a) The kinetics of calcite dissolution and precipitation in geologically relevant situations of karst areas: I Open-System. *Chem. Geol.* **48**, 189–211.

Buhmann D. and Dreybrodt W. (1985b) The kinetics of calcite dissolution and precipitation in geologically relevant situations of karst areas: II Closed-System. *Chem. Geol.* **53**, 109–124.

Corbel J. (1957) *Les Karsts du Nord-Ouest de l'Europe.* These d'Etat.

Curl R. L. (1973) Minimum diameter stalagmites. *Bull. Nat. Speleo. Soc.* **35**, 1–9.

Curtis J. (1884) Silver-lead deposits of Eureka, Nevada. *US Geol. Surv. Mon.* 7, 56–58

Drake J. J. (1980) The effect of soil activity on the chemistry of carbonate groundwater. *Water Resour. Res.* **16**, 381–386.

Drake J. J. (1983) The effects of geomorphology and seasonality on the chemistry of carbonate groundwaters. *J. Hydrol.* **61**, 223–226.

Dreybrodt W. (1980) Deposition of calcite from thin films of natural clacareous solutions and the growth of speleothems. *Chem. Geol.* **29**, 80–105.

Dreybrodt W. (1981) The kinetics of calcite deposition from thin films of natural clacareous solutions and the growth of speleothems: Revisited. *Chem. Geol.* **32**, 237–245.

Dreybrodt W. (1988) *Processes in Karst Systems.* Springer-Verlag.

Dreybrodt W. (1997) Chemical kinetics, speleothem growth, and climate. *Boreas* , xx–xx.

Dreybrodt W. and Buhmann D. (1987) A mass transfer model for dissolution and precipitation of calcite from solutions in turbulent motion. *Chem. Geol.* **90**, 107–122.

Dreybrodt W. and Franke H. W. (1987) Wachstumsgeschwindigkeiten und durchmesser von kerzenstalagmiten. *Die Hohle* **38**, 1–6.

Dreybrodt W., Eisenlohr B., Madry B., and Ringer S. (1998) Precipitation kinetics of calcite in the system $CaCO_3$-H_2O-CO_2: The conversion to CO_2 by the slow process $H^+ + HCO_3^- - CO_2 + H_2O$ and the inhibition of surface controlled reactions as rate limiting steps. *Geochim. Cosmochim. Acta* [ED UPDATE].

Ek C. and Gewelt M. (1985) Carbon dioxide in cave atmospheres. New results in Belgium and comparison with other countries. *Earth Surf. Procs. Landforms* **10**, 173–187.

Ford D. C. and Williams P. (1989) *Karst Hydrology and Geomorphology.* Chapman and Hall.

Franke H. W. (1965) The theory behind stalagmite shapes. *Stud. Speleo* **1**, 89–95.

Frasier S. (1996) TEM and SEM investigation of speleothem carbonates: Another key to the interpretation of environmental parameters. In *Climate Change; The Karst Record* (ed.); *Karst Waters Institute Spec. Pub.* **2**, 33–35.

Gams I. (1965) Uber die faktoren, die intensitat der sintersedimentation bestimmen. *Proc. Intl. Congr. Speleol.* **4**, 107–115.

Gams I. (1981) Contribution to morphometrics of stalagmite. *Proc. Intl. Congr. Speleol.* **8**, 276–278.

Genty D. (1992) Les speleothems du tunnel de Godarville (Belgique) - un exemple exceptionnel de concretionnement moderne - interet pour l'etude de la cinetique de precipitation de la calcite et de sa relation avec les variations d'environments. *Speleochronos* **4**, 3–29.

Genty D. (1993) Mise en evidence d'alternances saisonnieres dans la structure internedes stalagmites. Interet pour la reconstitution des paleoenvironments continentaux. *Acad. Sci. (Paris), Compt. Rendus II* **317**, 1229–1236.

Genty D. and Quinif Y. (1996) Annually laminated sequences in the internal structure of some Belgian stalagmites - importance for paleoclimatology. *J. Sediment. Petrol.* **66**, 275–288.

Genty D., Bastin B., and Ek C. (1995) Nouvel exemple d'alternances de lamines annuelles dans une stalagmite (Gtotte de Dinant la Merveilleuse, Belgique). *Speleochronos* **6**, 3–8.

Genty D., Baker A., and Barnes W. L. (1997) *Comparison entre les lamines luminescentes et les lamines visibles annuelles de stalagmites.* Compt. Rendus Acad. Sci.

Gonzalez L. A., Carpenter S. J., and Lohmann K. C. (1993) Columnar calcite in speleothems - Reply. *J. Sediment. Petrol.* **63**, 553–556.

Hovey H. C. (1896) *Celebrated American Caverns.* Robert Clarke and Co.

Kendall A. C. (1993) Columnar calcite in speleothems: Discussion. *J. Sediment. Petrol.* **63**, 550–552.

Kendall A. C. and Broughton P. L. (1978) Origin of fabrics in speleothems of columnar calcite crystals. *J. Sediment. Petrol.* **48**, 519–538.

Kirchmayer M. (1962) Zur untersuchung rezenter ooide. *Neues Jahrb. Geol. Palaontol.* **114**, 245–272.

Milne-Holme D. (1863) Notice of a large calcareous stalagmite brought from the Island of Bermuda in the year 1819 and now in the college of Edinburgh. *Royal Soc. Edinburgh Proc.* **5**, 423–428.

Orr P. C. (1952) Excavations in Moaning Cave. *Santa Barbara Mus. Nat. Hist. Anthropol. Bull.* **1**, 1–19.

Plummer L. N., Jones B. F., and Truesdell A. H. (1976) WATEQF - a FORTRAN IV version of WATEQ, a computer programme for calculating chemical equilibrium of natural waters. USGS Water Resour. Invest. 76–13.

Plummer L. N., Wigley T. L. M., and Parkhurst D. L. (1978) The kinetics of calcite dissolution in CO2-water systems at 5 –60°C and 0.00–1.0 atm. *Amer. J. Sci.* **278**, 537–573.

Price E. (1985) *The Bath Freestone Mines*. Free Troglophile Press.

Prinz W. (1908) Les cristallisations des grottes de Belgique. *Nouv. Mem. Soc. Belg. Geol.* **42.**

Railsback L. B., Brook G. A., Chen J., Kalin R., and Fleisher C. J. (1994) Environmental controls on the petrology of a late Holocene speleothem from Botswana with annual layers of aragonite and calcite. *J. Sediment. Res.* **A64,** 147–155.

Shopov Y. Y., Ford D. C., and Schwarcz H. P. (1994) Luminescent microbanding in speleothems: High resolution chronology and paleoclimate. *Geology* **22,** 407–410.

Sweeting M. M. (1972) *Karet Landforms*. Macmillan.